



HHS Public Access

Author manuscript

J Invest Dermatol. Author manuscript; available in PMC 2014 September 01.

Published in final edited form as:

J Invest Dermatol. 2014 March ; 134(3): 783–790. doi:10.1038/jid.2013.369.

Prognostic Impact of *PHIP* Copy Number in Melanoma: Linkage to Ulceration

Vladimir Bezrookove^{#1}, David De Semir^{#1}, Mehdi Nosrati¹, Schuyler Tong¹, Clayton Wu¹, Suresh Thummala¹, Altaf A. Dar¹, Stanley P.L. Leong¹, James E. Cleaver², Richard W. Sagebiel¹, James R. Miller III¹, and Mohammed Kashani-Sabet¹

¹Center for Melanoma Research and Treatment, California Pacific Medical Center and Research Institute, San Francisco, California,

²UCSF Helen Diller Family Comprehensive Cancer Center, San Francisco, California.

[#] These authors contributed equally to this work.

Abstract

Ulceration is an important prognostic factor in melanoma whose biologic basis is poorly understood. Here we assessed the prognostic impact of pleckstrin homology domain-interacting protein (*PHIP*) copy number and its relationship to ulceration. *PHIP* copy number was determined using fluorescence *in situ* hybridization (FISH) in a tissue microarray cohort of 238 melanomas. Elevated *PHIP* copy number was associated with significantly reduced DMFS ($P = 0.01$) and DSS ($P = 0.009$) by Kaplan-Meier analyses. *PHIP* FISH scores were independently predictive of DMFS ($P = 0.03$) and DSS ($P = 0.03$). Increased *PHIP* copy number was an independent predictor of ulceration status ($P = 0.04$). The combined impact of increased *PHIP* copy number and tumor vascularity on ulceration status was highly significant ($P < 0.0001$). Stable suppression of *PHIP* in human melanoma cells resulted in significantly reduced glycolytic activity *in vitro*, with lower expression of LDH5, HIF1A, and VEGF, and was accompanied by reduced microvessel density *in vivo*. These results provide further support for *PHIP* as a molecular prognostic marker of melanoma, and reveal a significant linkage between *PHIP* levels and ulceration. Moreover, they suggest that ulceration may be driven by increased glycolysis and angiogenesis.

Introduction

Melanoma is an important clinical problem, with an estimated 76,250 new cases and 9,180 deaths in 2012 (Siegel et al. 2012). The clinical behavior of melanoma can be unpredictable, making prognostic predictions difficult in individual patients. While tumor thickness consistently emerges as the single most significant prognostic factor determining survival, and while ulceration increases the risk of death within a given thickness range, additional

Users may view, print, copy, and download text and data-mine the content in such documents, for the purposes of academic research, subject always to the full Conditions of use:http://www.nature.com/authors/editorial_policies/license.html#terms

Corresponding Author: Mohammed Kashani-Sabet, MD; California Pacific Medical Center Research Institute; 475 Brannan Street, Suite 220, San Francisco, CA 94107 Telephone: (415) 600-3166; FAX: (415) 600-3865; kashani@cpmcri.org.

Conflict of Interest Mohammed Kashani-Sabet owns stock in Melanoma Diagnostics, Inc. Intellectual property covering the marker described in this study was licensed to Myriad Genetics Laboratories.

factors are required to refine the prognostic assessment of melanoma patients. Beyond histological factors that are reliably associated with decreased survival, molecular markers represent the next frontier in the evaluation of melanoma outcome. Despite the identification of numerous putative molecular prognostic factors, no prognostic biomarkers are routinely used in the evaluation of melanoma patients (Gogas et al. 2009). In addition, few biomarkers have been shown to retain prognostic impact, when measured on more than one platform (i.e., measurements at the DNA *versus* RNA *versus* protein level).

Recent studies performed by our group identified a previously unknown role for the pleckstrin homology domain-interacting protein (PHIP) in melanoma progression (De Semir et al. 2012). *PHIP* was identified as the top gene overexpressed in metastatic *versus* primary melanomas by gene expression profiling analysis (Haqq et al. 2005). shRNA-mediated suppression of *PHIP* resulted in significant suppression of melanoma cell invasion and metastatic potential in both murine and melanoma cell lines. High levels of PHIP expression were associated with significantly reduced survival in both mouse models and human tissues. Specifically, high PHIP expression (as determined by immunohistochemical analysis) was independently predictive of DMFS and DSS. In this study, we analyze the role of *PHIP* copy number for its prognostic significance in primary cutaneous melanoma and explore the linkage between PHIP levels and ulceration development in melanoma.

Results

Given the recent demonstration of a significant prognostic role for PHIP protein expression and the presence of elevated *PHIP* copy number in melanoma (De Semir et al. 2012), we aimed to determine the prognostic impact of *PHIP* copy number in primary cutaneous melanoma. *PHIP* copy number was analyzed using FISH on a TMA cohort of 238 specimens, with known immunohistochemical analysis of PHIP protein expression, by an observer blinded to patient outcomes. Overall, 22% of the cohort possessed a mean copy number of 3 or greater. See Figure 1a for representative examples of low *versus* high *PHIP* copy number. As the ratio of *PHIP* and probes representing the centromere of chromosome 6 in almost all of the cases was close to 1.0 (Table S1), the primary attribute assessed was percent of cells expressing 3 or more copies of the *PHIP* gene, in which there was a range from 0-87%, with a mean of 33.4%. There was a significant correlation between *PHIP* copy number and level of expression of the PHIP protein ($P < 0.0001$, Figure S1).

Initially, we analyzed the relationship between *PHIP* copy number and melanoma outcome using univariate analysis. High *PHIP* copy number was associated with decreased melanoma survival, when DMFS ($P = 0.01$ by log-rank test) and DSS ($P = 0.009$ by log-rank test) were assessed using Kaplan-Meier analysis (Figure 1b and 1c). In addition, there was a significantly increased risk of distant metastasis or death due to melanoma with the presence of high *PHIP* FISH scores. 45.4% of patients with high copy number had distant metastasis, when compared to 25.5% with low copy number (Fisher's exact test, $P = 0.015$). 42.2% of patients with high copy number died of metastatic melanoma, when compared to 17.7% of patients with low copy number (Fisher's exact test, $P < 0.002$).

Next, we examined the relationship between *PHIP* copy number and survival using multivariate Cox regression analysis. High *PHIP* FISH scores were significantly predictive of reduced DMFS ($P = 0.03$, Table 1) and DSS ($P = 0.027$, Table 2) in multivariate models that included tumor thickness, ulceration, age, gender, and tumor site. Thus, *PHIP* copy number was independently predictive of survival associated with melanoma, similar to the results obtained for PHIP protein expression (De Semir et al. 2012).

Recently, high PHIP immunohistochemical scores were shown to correlate with ulceration status (De Semir et al. 2012). We aimed to confirm this relationship at the DNA level. High *PHIP* copy number was significantly associated with ulceration status when analyzed by univariate logistic regression analysis ($P=0.004$). In addition, high *PHIP* copy number was associated with a significantly increased risk of developing ulceration. Thus, ulceration was present in 45.5% of cases with high *PHIP* copy number, when compared with 28.8% of cases with low *PHIP* copy number ($P = 0.013$, Fisher's exact test).

Previously, we reported that ulceration was associated with increased tumor vascularity in the primary tumor, when assessed morphologically (Kashani-Sabet et al. 2002). Elevated tumor vascularity (as determined by melanomas with prominent *versus* all lower degrees of vascularity) was significantly associated with ulceration status. Ulceration was present in 60.3% of the cases with prominent tumor vascularity, when compared with 22.2% of cases with lower degrees of tumor vascularity ($P < 0.0001$, Fisher's exact test). This served to confirm the previously reported results in this tissue microarray cohort. We then explored the combined impact of high *PHIP* copy number and elevated tumor vascularity on the development of ulceration. Ulceration was present in 20.2% of melanomas with both low *PHIP* copy number and low tumor vascularity. This increased to 38.8% of cases ulcerated with either prognostic factor elevated, and to 72.2% of melanomas ulcerated, when both factors were elevated ($P < 0.0001$, Chi-square test of percentage differences).

We then assessed the relationship between *PHIP* copy number and ulceration status, using multivariate logistic regression analysis. Presence of ulceration in melanoma is also known to increase both with increasing tumor thickness and with increasing mitotic rate (Balch et al. 2001b; Thompson et al. 2011). A multivariate logistic regression analysis was performed, including low *versus* high *PHIP* copy number, low *versus* high tumor vascularity, tumor thickness, and mitotic rate. All four factors were significantly predictive of the incidence of ulceration (Table 3). Thus, *PHIP* FISH scores were independently predictive of ulceration status, even with the inclusion of these other factors ($P = 0.04$).

Next, we explored cellular pathways regulated by PHIP expression potentially relevant to the development of ulceration. Targeted suppression of PHIP (using an anti-*PHIP* shRNA) in C8161.9 human melanoma cells (with elevated *PHIP* copy number) was previously shown to significantly suppress melanoma cell invasiveness and metastatic potential (De Semir et al. 2012). Given that PHIP functions in the IGF1R pathway that is important in regulating glucose metabolism, we assessed whether suppression of PHIP activity resulted in altered glycolytic activity of melanoma cells. C8161.9 cells expressing the anti-*PHIP* shRNA produced significantly lower amounts of lactate than control cells expressing a shRNA targeting luciferase (anti-*luc* shRNA) (Figure 2a). This was associated with

decreased expression of LDH5, the most efficient isoenzyme of lactate dehydrogenase, which catalyzes the conversion of pyruvate to lactate in the final step of glycolysis (Figure 2b). In addition, culturing anti-*PHIP* shRNA-expressing cells in the presence of methylpyruvate, which bypasses glycolysis and directly enters the Krebs cycle, resulted in significantly increased invasion (Figure 2c). Thus, the proinvasive role of PHIP in melanoma is mediated, at least in part, by activating the glycolytic pathway. Moreover, C8161.9 melanoma cells with reduced PHIP expression produced lower levels of VEGF, as determined by an ELISA assay of human VEGF secretion (Figure 2d). As VEGF expression is controlled by HIF1A (Forsythe et al. 1996), melanoma cells with suppressed PHIP expression were also shown to express lower levels of HIF1A by Western analysis (Figure 2b).

Finally, we assessed the effects of suppression of PHIP on the angiogenic potential of human melanoma cells *in vivo*. C8161.9 melanoma cells were inoculated subcutaneously into nude mice, and the resultant tumors examined for microvessel density using immunofluorescence of CD31 positivity. While there was no significant difference in the tumor volume between the two groups (data not shown), tumors in the anti-*PHIP* shRNA-expressing group (Figure 3a, right panel) exhibited large areas of necrosis when compared with the control group (Figure 3a, left panel). Analysis of CD31 expression revealed that the control tumors were characterized by large, abnormal blood vessels and hemorrhage, apparent from autofluorescence of erythrocytes and lipofuscin (Baschong et al. 2001) (Figure 3b and 3c, left panels). By contrast, the vessels in the anti-*PHIP* shRNA-expressing tumors were smaller, with little or no hemorrhage evident (Figure 3b and 3c, right panels). Finally, the anti-*PHIP* shRNA-expressing tumors had significantly reduced microvessel density when compared with the control tumors ($P < 0.02$ as assessed both by a T test and by a two-sample randomization test, Figure 3d). Thus, increasing PHIP expression in human melanoma cells promotes angiogenic potential.

Discussion

In this manuscript, we describe a previously unreported role for *PHIP* copy number in the prognosis associated with melanoma. *PHIP* FISH scores were predictive of a significantly increased risk of both distant metastasis and death due to melanoma, and were independently predictive of DMFS and DSS. In addition, elevated *PHIP* FISH scores were associated with a higher incidence of ulceration and were independently predictive of ulceration status. The combined impact of *PHIP* copy number and tumor vascularity was additive, as cases with high levels of both factors had a significantly higher incidence of ulceration than cases with low levels of either or both factors. Finally, C8161.9 human melanoma cells with suppressed PHIP expression exhibited reduced glycolytic activity and angiogenic potential.

These results provide further support for the role of PHIP as a molecular prognostic marker for melanoma, as initially described using immunohistochemical analysis of PHIP expression. High PHIP protein expression was associated with a significantly increased risk of distant metastasis and death due to melanoma, and was independently predictive of DMFS and DSS (De Semir et al. 2012). Our analysis of *PHIP* copy number parallels the

results obtained in human and murine melanoma cell lines, in which suppressed PHIP expression resulted in significantly reduced metastatic potential and increased survival in xenograft models.

To date, few markers have been shown to provide significant prognostic impact in melanoma when assessed on more than one platform. For example, *SPP1* expression has been shown to have independent prognostic significance when assessed at the RNA and protein levels (Rangel et al. 2008; Conway et al. 2009). Our studies have demonstrated a significant prognostic role for PHIP at both the DNA and protein levels. Although the ratio of *PHIP* to chromosome 6 centromeric probe was close to 1.0 in the great majority of cases examined, changes in *PHIP* copy number, ranging from euploidy to 3 or greater copies, were highly correlated with increased PHIP expression. Additional studies of PHIP levels will be required in distinct cohorts in order to further validate its prognostic role.

Beyond an independent impact on survival, these studies confirmed a significant and independent relationship between PHIP levels and ulceration status. In addition, *PHIP* copy number combined dramatically with tumor vascularity to increase the incidence of ulceration in primary melanoma specimens. Ulceration is an important prognostic factor that has been incorporated into the AJCC staging classification for melanoma for over a decade (Balch et al. 2001a, 2009). More recently, ulceration has been suggested as a potential predictive marker of benefit to adjuvant interferon alpha therapy (McMasters et al. 2010; Eggermont et al. 2012). However, the biologic basis for the development of ulceration is poorly understood.

Increasing incidence of ulceration in melanoma is associated with increasing tumor thickness, mitotic rate, and tumor vascularity (Balch et al. 2001b; Thompson et al. 2011). In addition, gene expression profiling studies have identified a gene signature that correlates with ulceration (Winnepeninckx et al. 2006). However, the specific cellular pathways and mechanisms by which ulceration develops are unclear. The linkage between PHIP levels and ulceration implies a role for the IGF1R pathway in ulceration, given PHIP's involvement in this signal transduction pathway. In addition, our studies in human melanoma cells demonstrating that downregulation of PHIP expression results in significantly reduced glycolytic activity, VEGF secretion, and microvessel density provide mechanistic insights, identifying glucose metabolism and tumor angiogenesis as pathways by which ulceration may develop in melanoma.

Tumor cell growth is promoted by increased glucose consumption, a phenomenon known as the Warburg effect (Warburg 1956). The importance of glycolysis to melanoma progression has been amply reported in melanoma cell lines (Halaban et al. 1997, 2002; Bagheri et al. 2006) and is demonstrated clinically by the utility of PET scanning in the radiologic assessment of melanoma both during initial staging (Reinhardt et al. 2006; Falk et al. 2007) and in response to targeted therapy (McArthur et al. 2012). Glycolysis in tumor cells is driven by AKT (Elstrom et al. 2004), and PHIP is a potent activator of AKT in melanoma (De Semir et al. 2012). Moreover, increased glucose metabolism can itself drive tumor angiogenesis, invasion, and metastasis (Lay et al. 2000; Tsutsumi et al. 2004). Thus, our studies on PHIP in melanoma describe a previously unreported link between PHIP, the

Warburg effect, tumor angiogenesis, and ulceration development. As PHIP is activated through increased copy number in a subset of melanomas, additional markers of ulceration will need to be identified in melanomas without PHIP activation. However, the mechanistic analyses provided here should facilitate the identification of these additional markers in distinct molecular subsets of melanoma patients.

Finally, our investigation of PHIP in melanoma tissues and cell lines suggests an intriguing link between ulceration and LDH levels. These results imply that a common tumor-promoting pathway (i.e., IGF1R), resulting in increased glycolysis, may underlie the biologic basis of two prominent prognostic markers incorporated into the AJCC staging classification, one that refines the prognosis of localized melanoma, the other the prognosis of disseminated melanoma. Elevated LDH5 expression in primary melanoma has been previously shown to be associated with reduced survival on univariate analysis, but was not independently predictive of melanoma outcome (Zhuang et al. 2010). Furthermore, LDH activity has been correlated to HIF1A expression and angiogenic potential (Koukourakis et al. 2003). However, further studies will be required in order to confirm the link between ulceration and LDH levels suggested by this analysis. In addition, high levels of angiopoietin-2 have been reported in multiple cancers, with a possible prognostic role (Bonner and Arbiser 2012), and are accompanied by upregulation of RAC signaling pathways (Felcht et al. 2012). Thus, it is possible that elevated PHIP copy number can modulate angiopoietin levels in melanoma, in part through mitochondrial dysfunction, NADPH oxidase induction, and increased generation of reactive oxygen species (which result in angiopoietin-2 activation). In conclusion, our studies support an important role for PHIP as a molecular marker of melanoma ulceration, metastasis and survival, and provide insights into the cellular pathways through which ulceration can develop.

Materials and methods

Study population

This study used a tissue microarray cohort that was previously described according to REMARK guidelines (Rangel et al. 2006; Kashani-Sabet et al. 2009). The molecular prognostic factor analyses performed herein were approved by the appropriate ethics boards both at CPMC and UCSF.

Fluorescence *in situ* hybridization (FISH)

FISH was performed as previously described (Wiegant and Raap 2001; Chin et al. 2003; De Semir et al. 2012) using BAC clones RP11-767O1, RP11-484L10, RP11-217L13 and CTD-2297E14 to detect the *PHIP* locus and clones RP11-26M18 and RP11-136K2 to detect 6q11.1 and 6p11.1 respectively (February 2009 freeze of the UCSC Genome Browser, <http://genome.ucsc.edu>). BAC DNA's were prepared with the Large-Construct kit (Qiagen, Valencia, CA) and labeled by nick translation with Alexa Fluor 488 and 594 dUTP's (Life Technologies, Grand Island, NY) as described (Wiegant and Raap 2001). The quality and mapping of all probes were verified by hybridization to normal metaphase spreads in combination with a commercially available centromeric probe for chromosome 6 (Open Biosystems, Lafayette, CO) before tissue analysis. Hybridization on TMA's was performed

as described previously (Wiegant and Raap 2001; Chin et al. 2003). Images were taken with a Zeiss Axio Imager Z2 controlled by AxioVision software. The FISH signals were assessed and counted manually from images with several Z stack layers acquired using a Zeiss Axio Image Z2 microscope controlled by AxioVision software (Zeiss, Jena, Germany). At least 30 nuclei from each case were evaluated, and the signals were interpreted according to guidelines described previously (Bayani and Squire 2004) and recorded as 1 through 5 or greater. Signals from BAC clones detecting 6q11.1 and 6p11.1 were interpreted as the centromeric signal for chromosome 6 and the count was used as control.

Cell culture studies

C8161.9 human melanoma cells stably expressing anti-*PHIP* shRNA and anti-*luciferase* (anti-*luc*) shRNA were generated and propagated as described (De Semir et al. 2012). Lactate production and invasion into matrigel were assayed as reported (De Semir et al. 2012). C8161.9 cells were treated with 10 mM methylpyruvate (Sigma, St. Louis, MO.) for 48 hours before the invasion assay. VEGF secretion was measured by using an ELISA kit following the manufacturer's instructions (DY293B, R&D Systems Inc, Minneapolis, MN). Western blotting was performed as described using antibodies targeting HIF1A (ab16066, Abcam, Minneapolis, MN), LDH5 (ab1015, Abcam) and GAPDH (MAB374, Millipore, Billerica, MA).

Immunofluorescence

Groups of 6 nu/nu mice were inoculated subcutaneously with 1 million C8161.9 human melanoma cells expressing either control *luc* or anti-*PHIP* shRNA. On day 25, the mice were euthanized and the tumors were assessed for microvessel density based on CD31 positivity by immunofluorescence, which was performed using a rabbit anti-CD31 antibody (ab28364, Abcam) and a secondary antibody labeled with Alexa Fluor 594 (Life Technologies) as described previously (Jalas et al. 2011). Mosaic images were acquired with 20X magnification at a fixed exposure with a Zeiss Axio Imager Z2 microscope controlled by AxioVision software. After automatically stitching the images, the number of CD31 positive objects and area were determined using ImageJ software. The number of CD31 positive vessels was quantitated and the microvessel density reported as the total CD31 count over the entire area of the tumor.

Statistical Analysis

Statistical methods used to assess the significance of various prognostic factors on melanoma outcome were previously described (Rangel et al. 2006; Kashani-Sabet et al. 2009). The coding for clinical or pathological attributes was performed as described by the AJCC staging committee for melanoma (Balch et al. 2001b). The correlation between *PHIP* copy number and immunohistochemical score was tested by regression analysis using Data Desk software. For both DMFS and DSS, the definition of high *PHIP* FISH scores, as measured by percentage of cells harboring 3 or more copies of *PHIP*, was established as equal to or greater than 16%. A 16% cutoff served to maximize the average of the sensitivity and specificity in the prediction of both DMFS and DSS, analyzed separately. The same 16% cutoff was then uniformly and consistently used in all subsequent analyses of DMFS

and DSS. The association between high *PHIP* copy number and DMFS or DSS was assessed using both Kaplan-Meier analysis and multivariate Cox regression. The association between high *PHIP* copy number and presence or absence of ulceration was assessed using both Fisher's exact test and multivariate logistic regression analysis. The association between a high degree of tumor vascularity and ulceration was also assessed using both Fisher's exact test and multivariate logistic regression. Assessment of the differential impacts of neither, either, and both of these two factors was done using both Chi-square analysis and Fisher's exact test. In predicting ulceration status, high *PHIP* copy number was uniformly defined as greater than or equal to 35% of tumor cells harboring 3 or more copies of the *PHIP* gene. This cutoff was similarly selected as the one that maximized the average of sensitivity and specificity in predicting ulceration. All *P* values reported are two-sided.

Supplementary Material

Refer to Web version on PubMed Central for supplementary material.

Acknowledgments

This work was supported by United States Public Health Service Grants CA114337 and CA122947 (to MKS), and by the Kay Charitable Trust. JEC is supported by the E.A. Dickson Emeritus Professorship and the Cancer Research Coordinating Committee of the University of California.

Abbreviations

PHIP	pleckstrin homology domain-interacting protein
FISH	fluorescence <i>in situ</i> hybridization
DMFS	distant metastasis-free survival
DSS	disease-specific survival
LDH5	Lactate dehydrogenase 5
VEGF	vascular endothelial growth factor
HIF1A	hypoxia inducible factor 1 alpha subunit
TMA	tissue microarray
shRNA	short hairpin RNA
CD31	cluster of differentiation 31
BAC	bacterial artificial chromosome
ELISA	Enzyme-Linked ImmunoSorbent Assay
IGF1R	insulin-like growth factor 1 receptor
RAC	RAS-related C3 botulinum toxin substrate
TIE	receptor tyrosine kinase epithelial-specific
NADPH oxidase	nicotinamide adenine dinucleotide phosphate-oxidase

References

- Bagheri S, Nosrati M, Li S, et al. Genes and pathways downstream of telomerase in melanoma metastasis. *Proc Natl Acad Sci USA*. 2006; 103:11306–11. [PubMed: 16847266]
- Balch CM, Buzaid AC, Soong SJ, et al. Final version of the American Joint Committee on Cancer staging system for cutaneous melanoma. *J Clin Oncol*. 2001a; 19:3635–48. [PubMed: 11504745]
- Balch CM, Gershenwald JE, Soong S-J, et al. Final version of 2009 AJCC melanoma staging and classification. *J Clin Oncol*. 2009; 27:6199–206. [PubMed: 19917835]
- Balch CM, Soong SJ, Gershenwald JE, et al. Prognostic factors analysis of 17,600 melanoma patients: validation of the American Joint Committee on Cancer melanoma staging system. *J Clin Oncol*. 2001b; 19:3622–34. [PubMed: 11504744]
- Baschong W, Suetterlin R, Laeng RH. Control of Autofluorescence of Archival Formaldehyde-fixed, Paraffin-embedded Tissue in Confocal Laser Scanning Microscopy (CLSM). *J Histochem Cytochem*. 2001; 49:1565–71. [PubMed: 11724904]
- Bayani J, Squire JA. Fluorescence in situ Hybridization (FISH). *Curr Protoc Cell Biol*. 2004 Chapter 22: Unit 22.4.
- Bonner MY, Arbiser JL. Targeting NADPH oxidases for the treatment of cancer and inflammation. *Cell Mol Life Sci*. 2012; 69:2435–42. [PubMed: 22581366]
- Chin S-F, Daigo Y, Huang H-E, et al. A simple and reliable pretreatment protocol facilitates fluorescent in situ hybridisation on tissue microarrays of paraffin wax embedded tumour samples. *MP, Mol Pathol*. 2003; 56:275–9. [PubMed: 14514921]
- Conway C, Mitra A, Jewell R, et al. Gene expression profiling of paraffin-embedded primary melanoma using the DASL assay identifies increased osteopontin expression as predictive of reduced relapse-free survival. *Clin Cancer Res*. 2009; 15:6939–46. [PubMed: 19887478]
- Eggermont AMM, Suci S, Testori A, et al. Ulceration and stage are predictive of interferon efficacy in melanoma: results of the phase III adjuvant trials EORTC 18952 and EORTC 18991. *Eur J Cancer*. 2012; 48:218–25. [PubMed: 22056637]
- Elstrom RL, Bauer DE, Buzzai M, et al. Akt stimulates aerobic glycolysis in cancer cells. *Cancer Res*. 2004; 64:3892–9. [PubMed: 15172999]
- Falk MS, Truitt AK, Coakley FV, et al. Interpretation, accuracy and management implications of FDG PET/CT in cutaneous malignant melanoma. *Nucl Med Commun*. 2007; 28:273–80. [PubMed: 17325590]
- Felcht M, Luck R, Schering A, et al. Angiopoietin-2 differentially regulates angiogenesis through TIE2 and integrin signaling. *J Clin Invest*. 2012; 122:1991–2005. [PubMed: 22585576]
- Forsythe JA, Jiang BH, Iyer NV, et al. Activation of vascular endothelial growth factor gene transcription by hypoxia-inducible factor 1. *Mol Cell Biol*. 1996; 16:4604–13. [PubMed: 8756616]
- Gogas H, Eggermont AMM, Hauschild A, et al. Biomarkers in melanoma. *Ann Oncol*. 2009; 20(Suppl 6):vi8–13. [PubMed: 19617299]
- Halaban R, Cheng E, Zhang Y, et al. Aberrant retention of tyrosinase in the endoplasmic reticulum mediates accelerated degradation of the enzyme and contributes to the dedifferentiated phenotype of amelanotic melanoma cells. *Proc Natl Acad Sci USA*. 1997; 94:6210–5. [PubMed: 9177196]
- Halaban R, Patton RS, Cheng E, et al. Abnormal acidification of melanoma cells induces tyrosinase retention in the early secretory pathway. *J Biol Chem*. 2002; 277:14821–8. [PubMed: 11812790]
- Haqq C, Nosrati M, Sudilovsky D, et al. The gene expression signatures of melanoma progression. *Proc Natl Acad Sci USA*. 2005; 102:6092–7. [PubMed: 15833814]
- Jalas JR, Vemula S, Bezrookove V, et al. Metastatic melanoma with striking adenocarcinomatous differentiation illustrating phenotypic plasticity in melanoma. *Am J Surg Pathol*. 2011; 35:1413–8. [PubMed: 21836492]
- Kashani-Sabet M, Sagebiel RW, Ferreira CMM, et al. Tumor vascularity in the prognostic assessment of primary cutaneous melanoma. *J Clin Oncol*. 2002; 20:1826–31. [PubMed: 11919240]
- Kashani-Sabet M, Venna S, Nosrati M, et al. A multimarker prognostic assay for primary cutaneous melanoma. *Clin Cancer Res*. 2009; 15:6987–92. [PubMed: 19887476]

- Koukourakis MI, Giatromanolaki A, Sivridis E, et al. Lactate dehydrogenase-5 (LDH-5) overexpression in non-small-cell lung cancer tissues is linked to tumour hypoxia, angiogenic factor production and poor prognosis. *Br J Cancer*. 2003; 89:877–85. [PubMed: 12942121]
- Lay AJ, Jiang XM, Kisker O, et al. Phosphoglycerate kinase acts in tumour angiogenesis as a disulphide reductase. *Nature*. 2000; 408:869–73. [PubMed: 11130727]
- McArthur GA, Puzanov I, Amaravadi R, et al. Marked, homogeneous, and early [18F]fluorodeoxyglucose-positron emission tomography responses to vemurafenib in BRAF-mutant advanced melanoma. *J Clin Oncol*. 2012; 30:1628–34. [PubMed: 22454415]
- McMasters KM, Edwards MJ, Ross MI, et al. Ulceration as a predictive marker for response to adjuvant interferon therapy in melanoma. *Ann Surg*. 2010; 252:460–465. discussion 465–466. [PubMed: 20739846]
- Rangel J, Nosrati M, Torabian S, et al. Osteopontin as a molecular prognostic marker for melanoma. *Cancer*. 2008; 112:144–50. [PubMed: 18023025]
- Rangel J, Torabian S, Shaikh L, et al. Prognostic significance of nuclear receptor coactivator-3 overexpression in primary cutaneous melanoma. *J Clin Oncol*. 2006; 24:4565–9. [PubMed: 17008696]
- Reinhardt MJ, Joe AY, Jaeger U, et al. Diagnostic performance of whole body dual modality 18F-FDG PET/CT imaging for N- and M-staging of malignant melanoma: experience with 250 consecutive patients. *J Clin Oncol*. 2006; 24:1178–87. [PubMed: 16505438]
- De Semir D, Nosrati M, Bezrookove V, et al. Pleckstrin homology domain-interacting protein (PHIP) as a marker and mediator of melanoma metastasis. *Proc Natl Acad Sci USA*. 2012; 109:7067–72. [PubMed: 22511720]
- Siegel R, Naishadham D, Jemal A. Cancer statistics, 2012. *CA Cancer J Clin*. 2012; 62:10–29. [PubMed: 22237781]
- Thompson JF, Soong S-J, Balch CM, et al. Prognostic significance of mitotic rate in localized primary cutaneous melanoma: an analysis of patients in the multi-institutional American Joint Committee on Cancer melanoma staging database. *J Clin Oncol*. 2011; 29:2199–205. [PubMed: 21519009]
- Tsutsumi S, Yanagawa T, Shimura T, et al. Autocrine motility factor signaling enhances pancreatic cancer metastasis. *Clin Cancer Res*. 2004; 10:7775–84. [PubMed: 15570012]
- Warburg O. On the origin of cancer cells. *Science*. 1956; 123:309–14. [PubMed: 13298683]
- Wiegant J, Raap AK. Probe labeling and fluorescence in situ hybridization. *Curr Protoc Cytom*. 2001 Chapter 8: Unit 8.3.
- Winnepenninckx V, Lazar V, Michiels S, et al. Gene expression profiling of primary cutaneous melanoma and clinical outcome. *J Natl Cancer Inst*. 2006; 98:472–82. [PubMed: 16595783]
- Zhuang L, Scolyer RA, Murali R, et al. Lactate dehydrogenase 5 expression in melanoma increases with disease progression and is associated with expression of Bcl-XL and Mcl-1, but not Bcl-2 proteins. *Mod Pathol*. 2010; 23:45–53. [PubMed: 19838163]

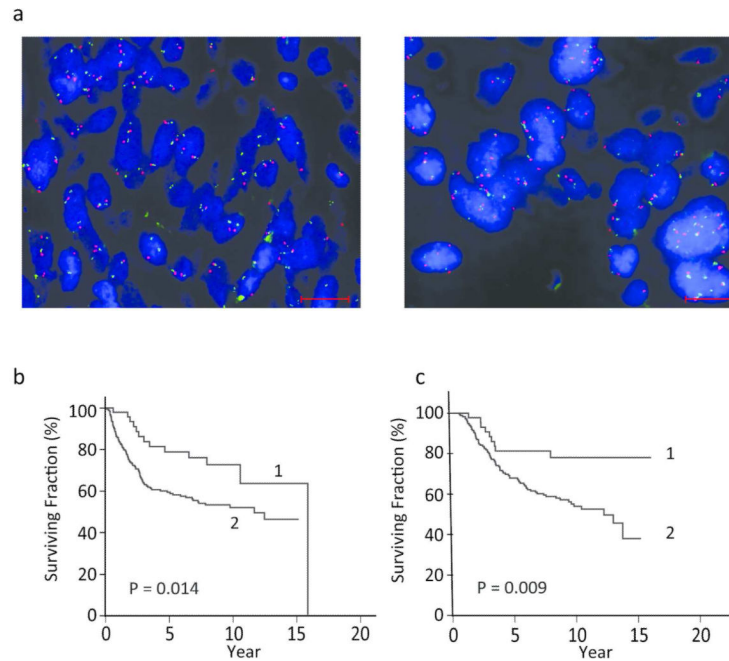


Figure 1. *PHIP* copy number and its correlation with DMFS and DSS in melanoma patients. (a) Dual color FISH for *PHIP* locus, red, and centromere of chromosome 6, green, representative of low *PHIP* copy number, left panel, and high copy number, right panel. Scale bar = 20 Rm. (b) Kaplan-Meier analysis of DMFS in patients with low *PHIP* copy number (curve 1) versus patients with high *PHIP* copy number (curve 2). (c) Kaplan-Meier analysis of DSS in patients with low *PHIP* copy number (curve 1) versus patients with high *PHIP* copy number (curve 2).

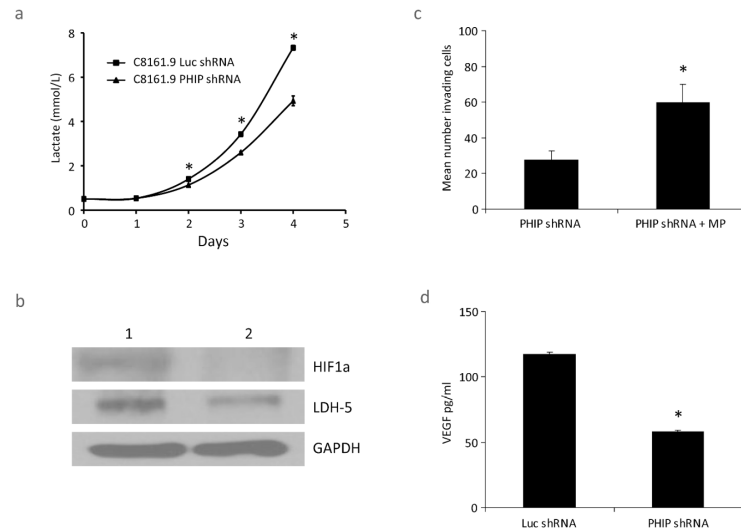
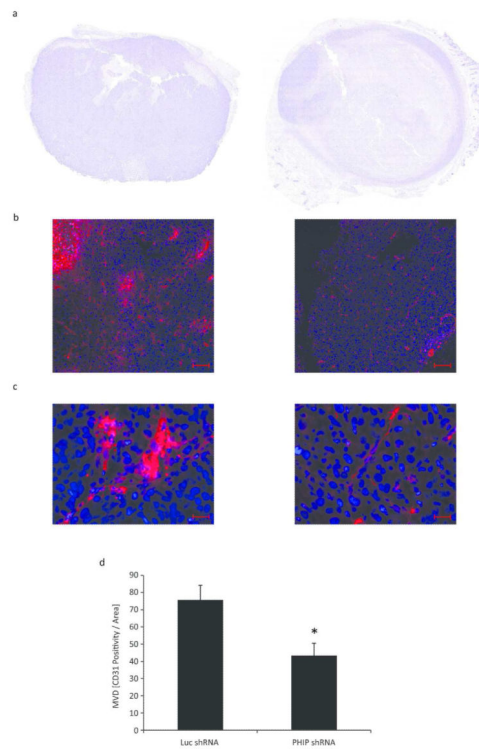


Figure 2.

Effects of shRNA-mediated suppression of PHIP in human melanoma cells. (a) Lactate production in C8161.9 cells expressing anti-*PHIP* shRNA versus control cells expressing anti-*luc* shRNA. Mean \pm SE; N = 3. * denotes $P < 0.003$. (b) Western analysis of LDH5 and HIF1A in C8161.9 cells expressing anti-*luc* shRNA (control cells, lane 1) or anti-*PHIP* shRNA (lane 2). (c) Invasive capacity of C8161.9 stable transformants expressing anti-*PHIP* shRNA with or without the addition of methylpyruvate (MP). Mean \pm SE; N = 3. * denotes $P < 0.05$. (d) ELISA assay of human VEGF levels produced by C8161.9 cells expressing anti-*PHIP* shRNA versus control cells expressing anti-*luc* shRNA. Mean \pm SE; N = 3. * denotes $P < 0.0001$.

**Figure 3.**

Effects of PHIP expression on the angiogenic potential of C8161.9 human melanoma cells *in vivo*. (a) Representative images of H&E staining of subcutaneous tumors in nude mice. The left panel shows the growth pattern of C8161.9 cells expressing anti-*luc* shRNA, compared with C8161.9 cells expressing anti-*PHIP* shRNA (right panel). (b) Composite images of immunofluorescence detection of CD31, red, and DAPI, blue as counterstain. The left panel shows the staining pattern of CD31 in subcutaneous tumor with C8161.9 cells expressing anti-*luc* shRNA compared with C8161.9 cells expressing anti-*PHIP* shRNA (right panel). Scale bar = 100 Rm. (c) Composite images of CD31 staining pattern with higher magnification for tumors with C8161.9 cells expressing anti-*luc* shRNA (left panel), or anti-*PHIP* shRNA (right panel). Scale bar = 20 Rm. (d) Quantification of microvessel density (MVD) based on CD31 immunofluorescence positivity in tumors (six per group) with C8161.9 cells expressing either anti-*luc* shRNA or anti-*PHIP* shRNA. Mean \pm SD. * denotes $P < 0.02$.

Table 1

Cox regression analysis of impact of various prognostic factors on DMFS of melanoma cohort (N = 231).

Prognostic factor	Chi-square	Risk Ratio	P value
Tumor thickness	6.96	1.38	.008
High <i>PHIP</i> copy number	4.73	1.99	.03
Ulceration	3.31	1.51	.07
Sex	1.41	1.34	.24
Site	0.92	1.24	.34
Age	0.61	0.95	.44

Author Manuscript

Author Manuscript

Author Manuscript

Author Manuscript

Table 2

Cox regression analysis of impact of various prognostic factors on DSS of melanoma cohort (N = 231).

Prognostic factor	Chi-square	Risk Ratio	P value
Tumor thickness	6.13	1.38	.013
High <i>PHIP</i> copy number	4.87	2.21	.027
Ulceration	3.63	1.58	.057
Sex	1.00	1.30	.32
Site	0.81	1.24	.37
Age	0.01	0.99	.91

Author Manuscript

Author Manuscript

Author Manuscript

Author Manuscript

Table 3

Logistic regression analysis of impact of various prognostic factors on incidence of ulceration in melanoma cohort (N = 228).

Prognostic factor	Chi-square	Odds Ratio	P value
Mitotic rate	15.24	1.23	.0001
Tumor vascularity	10.26	3.05	.001
Tumor thickness	5.99	1.63	.01
High <i>PHIP</i> copy number	4.10	1.96	.04

Author Manuscript

Author Manuscript

Author Manuscript

Author Manuscript